Structures and Buildings

Finite-element analyses of light timber-framed walls with and without openings
Togay, Anil, Karagöz Işleyen, Ediz and Durucan
ice | proceedings

Proceedings of the Institution of Civil Engineers

http://dx.doi.org/10.1680/jstbu.16.00085
Paper 1600085
Received 13/04/2016 Accepted 21/02/2017
Keywords: buildings, structures & design/ strength & testing of materials/timber structures

ice Institution of Civil Engineers
publishing

Finite-element analyses of light timber-framed walls with and without openings

1 **Abdullah Togay** PhD
Associate Professor, Department of Industrial Design, Gazi University, Ankara, Turkey

2 **Özgür Anil** PhD
Professor, Civil Engineering Department, Gazi University, Ankara, Turkey (corresponding author: oanil@gazi.edu.tr)

3 **Ümmü Karagöz Işleyen** PhD
Assistant Professor, Department of Wood Products Industrial Engineering, Kastamonu University, Kastamonu, Turkey

4 **İbrahim Ediz** MSc
PhD Student, Gazi University, Ankara, Turkey; Computer Engineer, Ministry of Education, Ankara, Turkey

5 **Cengizhan Durucan** PhD
Assistant Professor, Civil Engineering Department, Ahievran University, Kırşehir, Turkey





The static responses of timber-framed shear walls with and without openings of variable dimensions and locations were numerically investigated using the finite-element (FE) method. The lateral load resistance capacities and general load–displacement behaviours of the timber-framed shear walls were investigated. In the FE study, the frame elements were modelled as beams, plates were modelled as shells and nails were modelled as spring elements. The plastic behaviour of the materials was modelled using experimental stress–strain relationships of the materials. For timber frames and oriented strand board (OSB) panels, uniaxial stress–strain curves were experimentally obtained under tensile and compressive loading. From the experimental materials models it was found that spruce exhibited non-linear behaviour under both tensile and compressive stress. In contrast, the OSB sheathing layer used in the analyses exhibited non-linear behaviour under compressive stress and linear behaviour under tensile stress. The numerical results were verified using experimental load–deflection relationships obtained from a previous study. Good agreement was found between the analytical and experimental results. To further examine the applicability of the experimentally verified numerical model, four different timber-framed shear walls were simulated with FE models.

Notation

A_0	sum of opening areas
d	fastener diameter
E	elastic modulus
F	strength and stiffness ratio
G	shear modulus
H	wall height
K_{ser}	slip modulus of connection at the serviceability limit state (N/mm)
K_u	slip modulus of connection at the ultimate limit state (N/mm)
L	wall width
L_i	width of full-height sheathing wall
r	opening coefficient
α	opening area ratio
β	wall length ratio
$\varepsilon_{plastic}$	strain at initial yield
v	Poisson's ratio
ρ_m	mean density (kg/m^3)
$\rho_{m,1}$	density of wood frame (spruce, 420 kg/m^3)
$\rho_{m,2}$	density of sheathing panel (OSB, 590 kg/m^3)
σ	stress at initial yield

1. Introduction

Generally, timber structures exhibit good earthquake performance due their high strength to weight ratios (Premrov and Dobrila, 2012) and they are thus widely used in the construction industry worldwide. In the USA, Canada, Continental Europe and Japan, a significant amount of people conduct their daily lives in timber structures. In timber structures with one or more storey, timber-framed wall elements with lateral load resistance capacities are used. Timber structures are competitive among other type of structures and offer advantages in terms of meeting social and environmental requirements such as rapid construction times, low energy consumption and high safety under ground motion excitations (Premrov and Dobrila, 2012).

Light timber-framed walls are composed of frames, surface covering plates and connecting or fastening elements. The contribution of the frame elements to the load-resisting mechanism is in the vertical direction. The horizontal load resistance of timber-framed shear walls is generally provided by the surface covering panels. In addition, the linking elements in the connection points also contribute to the energy dissipation capacity and the ductility ratio of timber-framed panel walls (Šilih *et al*., 2012).

Many experimental studies have been conducted to measure the earthquake performance of light timber-framed walls in recent years (Anıl *et al*., 2016; Ayoub, 2007; Boudaud *et al*., 2015; Folz and Filiatrault, 2001; Premrov and Kuhta, 2008, 2010). However, the accurate modelling of timber-framed shear panels in experimental studies, including important factors such as dimensions, support and loading conditions, is very expensive and time consuming. To this end, finite-element (FE) modelling strategies have been developed to numerically simulate light timber-framed walls. In order to develop and verify such FE models, results from the available experimental studies have generally been used. Consequently, the experimentally verified timber-framed panel wall models are used to simulate the behaviour of such panels without conducting any experiments (Casagrande *et al*., 2016; Källsner and Girhammar, 2009).

Several structural models to simulate the behaviour of linking elements and panels have been proposed (Humbert *et al*., 2014; Judd and Fonseca, 2005; Polensek, 1976; Xu and Dolan, 2009a). The main focus in these studies was the linking elements, which significantly affect structural behaviour, and simplified load–displacement relationships for these linking elements have been presented (Andreasso *et al*., 2002; Meghlat *et al*., 2013). Such relationships are generally based on coupon tests. Furthermore, constitutive laws used to simulate the hysteretic behaviour of widely used linking elements in timber structures (i.e. nails, screws, staples, elbow-type three-dimensional (3D) connectors, perforated plates) have been developed for use in FE simulations (Humbert *et al*., 2014; Xu and Dolan, 2009b). In these studies, three main modelling techniques were used. These are

- techniques based on linear elastic or elasto-plastic beam theory (Blasetti *et al*., 2008; Šilih *et al*., 2012)
- techniques implementing the use of simplified springs, in the location of nails or screws, with linear and non-linear force–deformation characteristics (Valipour *et al*., 2014; Xu *et al*., 2012)
- FE methods implementing the use of 3D solid elements accounting for the friction between timber and linking elements (i.e. nails or screws) (Boudaud *et al*., 2015; Folz and Filiatrault, 2001; Meghlat *et al*., 2013).

One of the most significant issues in FE modelling of timber-framed panels is the accurate modelling of material properties (Bolmsvik *et al*., 2014). Generally, in FE studies, the frame elements are modelled as beams, plates are modelled as shells and nails are modelled as spring elements (Ayoub, 2007; Folz and Filiatrault, 2001; Foschi, 1977; Pang and Rosowsky, 2010; Polensek, 1976; Richard *et al*., 2002). The diagonal strut approach is used as another alternative in the mathematical and FE modelling of timber panels (Pintaric and Premrov, 2013). In FE analyses, timber frame elements with a heterogeneous structure and surface covering plates are generally modelled as orthotropic materials (Andreasso *et al*., 2002; Baylor and Harte, 2013; Guan and Zhu, 2009; Valipour *et al*., 2014).

This study is focused on the FE modelling of shear panels contributing to the lateral strength in timber-framed structures. In the work reported here, FE models of experimentally tested wall panels with and without openings were developed and the numerical results were compared with experimental data (Anıl *et al*., 2016). Force-controlled analyses of timber shear walls were conducted to obtain the load–displacement relationships, stress distributions and rate of damage to the panels. Moreover, the developed FE model was used to simulate the behaviour of four different models without experimental verification. Finally, by using the experimentally verified FE model, an equation was developed to estimate the effect of openings on the load-resisting capacities of timber-framed walls.

2. Experimental study

Timber-framed panel walls were tested under lateral, reverse cyclic loading to simulate ground motion excitations. In total, 11 timber-framed panel walls were tested in the scope of this study. The test specimens were manufactured to real dimensions, without any scaling. The main variables considered were the aspect ratios of the timber-framed panel walls, the presence of lateral retrofitted elements distributed along the height of the panel and the dimensions of openings in the panel walls. The properties of the test specimens are presented in Table 1 (Anıl *et al*., 2016).

The timber-framed panel walls were composed of timber frame elements and oriented strand board (OSB) used to sheet the surface of the wall. The production of test elements began with the formation of a frame of spruce elements of dimensions 38×140 mm. To join the spruce frame elements, two no. 10 wood screws (5×100 mm) were used for the lower and upper horizontal pieces and two no. 10 wood screws were used to join the vertical side and central pieces. Nails ($3{\cdot}1 \times 80$ mm) were used to join the OSB surface sheathing material to the timber frame elements. A pneumatic nail-driving machine was used to speed up the process. The nails were placed at 100 mm intervals on the external edges of the timber frame and at 300 mm intervals on the perpendicular and horizontal elements of the central section. The production of panels was completed when both sides were covered by OSB of 11 mm thickness. The elements and components that formed the

Table 1. Specimen properties

Specimen	Timber wall width/height: mm	Width/height ratio	Opening area ratio: %[a]	Lateral bracing	Timber wall configuration
1	1258/2650	0·47	0	No	
2	2372/2650	0·90	33	No	
3	1868/2650	0·70	0	No	
4	1868/2650	0·70	0	Yes	
5	2972/2650	1·12	28	No	
6	2478/2650	0·94	0	No	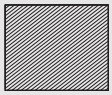
7	2478/2650	0·94	0	Yes	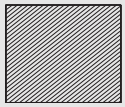
8	648/2650	0·24	0	No	
9	1772/2650	0·67	3	No	
10	2772/2650	1·05	27	No	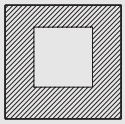
11	2142/2650	0·81	28	No	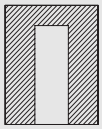

[a]Ratio of opening area to full area of timber-framed shear wall

standard timber-framed shear wall are shown in Figure 1 and some photographs taken during the construction of test specimens are given in Figure 2 (Anıl *et al.*, 2016).

Experiments were conducted under reverse cyclic loading to simulate ground motion excitation. Steel support plates were used to attach and fix the specimens onto a reinforced concrete rigid test platform. Loading was exerted by means of a loading column placed between a reinforced concrete rigid wall and the test specimens. Loading was applied to the test specimens with a 400 kN capacity hydraulic jack and measured with a load cell. A special system to prevent out-of-plane movement was designed and produced from structural steel and the horizontal load applied to the test specimens remained in the plane of the timber-framed shear walls. Horizontal sticks with bearings located between the test specimens and the frame eliminated the negative effects of friction (Anıl *et al.*, 2016).

Electronic deformation measurements of the displacements occurring in the test specimens were measured and transferred, with a data logger, to a computer and stored for later

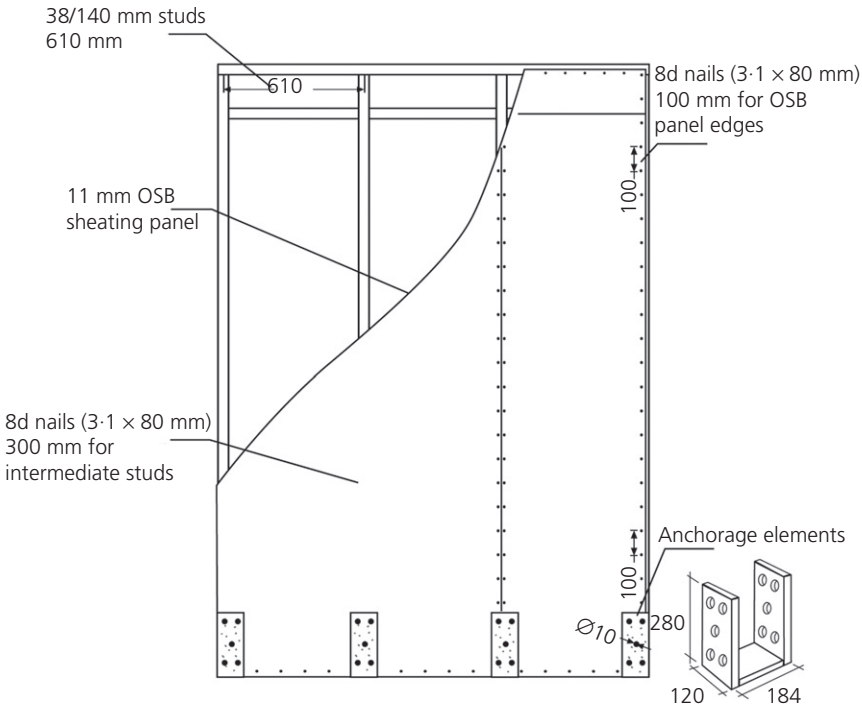

Figure 1. Schematic illustration of standard timber-framed shear wall (dimensions in mm)

Figure 2. Manufacturing process of test specimens

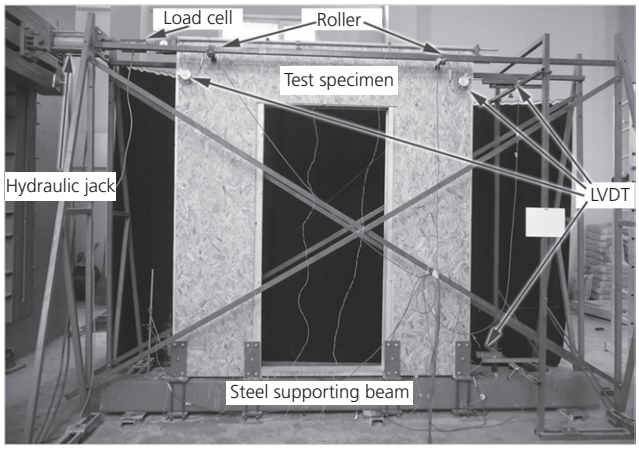

Figure 3. Test setup and instrumentation

evaluation. The measurements taken from the test specimens were horizontal storey displacement, rigid body turning, sliding, and shear displacement on the OSB. In addition to the displacement measurements, strain measurements of horizontal and perpendicular timber elements were also taken. A view of the experimental setup is provided in Figure 3 (Anıl *et al.*, 2016).

3. Finite-element model

Ansys version 14 was used to perform the numerical study on the lateral cyclic behaviour of the wood-framed shear walls. The predicted responses of the timber-framed shear walls were then compared with experimental results.

3.1 Element types and material properties

The timber-framed shear wall specimens consisted of several materials (wood, OSB sheathing panels and mechanical fasteners (nails and screws)). In the FE analyses, the frame elements were modelled as beams, plates were modelled as shells and nails were modelled as spring elements.

The Beam188 element used in the modelling of timber frame elements is based on Timoshenko beam theory and has six degrees of freedom (i.e. translations and rotations in the x, y and z directions) in each node.

Shell181, used to simulate the behaviour of the surface covering plates, is 2D without any actual thickness. However, it is capable of simulating 3D behaviour. Shell181 has four nodes and has six degrees of freedom (i.e. translations and rotations in the x, y and z directions) in each node.

The Combin14 element, used to simulate the behaviour of nails, is a spring element with a spring dashpot property and unidirectional tension–compression behaviour. This element has three degrees of freedom (i.e. translations in the x, y and z directions) in each node. The longitudinal spring element stiffness and damping coefficient are used to define the mechanical properties of this element.

In general, such linking elements exhibit an initially small linear sliding behaviour. However, the stiffness of the linking element decreases with increasing load levels, causing non-linear behaviour. In standard procedures, the linking elements are generally simulated with linear elastic type behaviour (Šilih *et al.*, 2012). However, in this study, for design requirements, the non-linear behaviour was simulated through two values of the slip modulus, K_{ser} at the serviceability limit state and K_u at the ultimate limit state (Meghlat *et al.*, 2013).

The axial modulus of stiffness of the nails connecting the frame and the OSB panels was calculated using the method given in Eurocode5 (CEN, 2010) (Equations 1–3). In the equations, the slip modulus in the elastic range for nails without pre-drilling is K_{ser} and K_u is the post-elastic slip modulus of nails until the maximum load.

1. $$K_{ser} = \frac{\rho_m^{1.5} \times d^{0.8}}{30}$$

2. $$\rho_m = \sqrt{\rho_{m,1} \times \rho_{m,2}}$$

3. $$K_u = \frac{2}{3} K_{ser}$$

The stiffness values of the nails used in the FE simulations thus calculated were $K_{ser} = 458$ N/mm and $K_u = 612$ N/mm, respectively.

In the FE analyses of the timber frame panels, the timber frame elements and the OSB panels were modelled as non-linear materials with orthotropic and elasto-plastic properties (Andreasso *et al.*, 2002; Guan and Zhu, 2009; Valipour *et al.*, 2014). The density, modulus of elasticity in the longitudinal, radial and tangential directions, shear modulus and Poisson's ratio of spruce and the OSB sheathing layer were obtained from previously conducted studies (Baylor and Harte, 2013; Guan and Zhu, 2009; Zhu *et al.*, 2005). The material properties used in the FE analyses are given in Table 2.

The plastic behaviour of the materials was modelled using the experimental stress–strain relationships. For the timber frames and OSB panels, uniaxial stress–strain curves were experimentally obtained under tensile and compressive loading. From these stress–strain relationships, it was found that spruce (used as the timber frame material) exhibited non-linear behaviour under both tensile and compressive stress. On the contrary, the

Table 2. Material properties used for FEA

	Spruce	OSB
Density: kg/m^3	420	590
Elastic modulus x direction, E_x: MPa	11 000	3500
Elastic modulus y direction, E_y: MPa	900	1585
Elastic modulus z direction, E_z: MPa	500	130
Shear modulus of xy plane, G_{xy}: MPa	676	500
Shear modulus of yz plane, G_{yz}: MPa	57	50
Shear modulus of xz plane, G_{xz}: MPa	636	100
Poisson's ratio of xy plane, ν_{xy}	0·37	0·184
Poisson's ratio of yz plane, ν_{yz}	0·47	0·312
Poisson's ratio of xz plane, ν_{xz}	0·42	0·364
Tensile strength: MPa	36·82	6·77
Compression strength: MPa	55	14·19

OSB sheathing layer used in the analyses exhibited non-linear behaviour under compressive stress and linear behaviour under tensile stresses. The tension tests on the spruce were conducted as per TS 2475 (TSE, 1976). The compressive stress–strain curves of the OSB sheathing layer were obtained as per ASTM D3501-05a (ASTM, 2011). The stress–strain curves of spruce (in tension) and OSB panels (in compression) are given in Figure 4. The multi-linear kinematic hardening model was used to simulate the plastic behaviour of the timber and OSB materials.

As noted earlier, in the FE simulations, the nails were simulated with Combin14 (spring with dashpot) from the Ansys library. Combin14 is a special spring element with different stiffness values in tension and compression. The nails between the OSB and the timber frame were defined with this element and no other stress–strain relationship was defined for the nails. The stiffness coefficients used with Combin14 were calculated as per Eurocode5 (CEN, 2010) (Equations 1–3).

According to the input data format required by the FE analysis package Ansys, the yield stresses on the stress–strain curve should be implemented together with their corresponding values of equivalent plastic strain. This is zero at the initial yield and equal to the total strain minus the elastic strain at subsequent yield points (Equation 4)

$$\varepsilon_{\text{plastic}} = \varepsilon_{\text{total}} - \frac{\sigma}{E} \quad (4)$$

3.2 Mesh

In FE modelling, continuous bodies are divided into smaller elements to obtain more accurate results. An increased number of these small elements increases the accuracy of the results, but the computational time and effort significantly increase with increasing numbers of elements. In order to determine the optimum number of elements, mesh sensitivity analyses are required. From the mesh sensitivity analysis conducted (Figure 5), the optimum element size was selected as 40 mm.

In Figure 5, the horizontal axis (i.e. the x axis) gives the number of elements and the vertical axis (the y axis) gives the horizontal displacement of the top point of the frame. As can be seen in Figure 5, increasing the number of elements from 10 000 to 15 000 led to only a negligible increase in the displacement value. Based on this negligible increase, it was decided that using more than 15 000 elements would be unnecessary. In relation to having at least 15 000 elements, the minimum size of the elements was determined to be 40 mm. The use of elements with smaller dimensions was considered unnecessary to perform accurate and computationally efficient analyses.

3.3 Boundary conditions and load

The connection of the timber panels to the rigid ground was provided by steel linking elements to prevent the slip and rotation of the panels. In the FE analyses, such linking points are assigned with fixed-support properties (i.e. constraining any translational or rotational movement). Lateral loading was applied by modelling a steel part similar in dimensions to the loading arm in the experimental setup. Reverse cyclic loading was applied in an incremental manner with 5 kN load increments. The support and loading conditions of the panels are given in Figure 6.

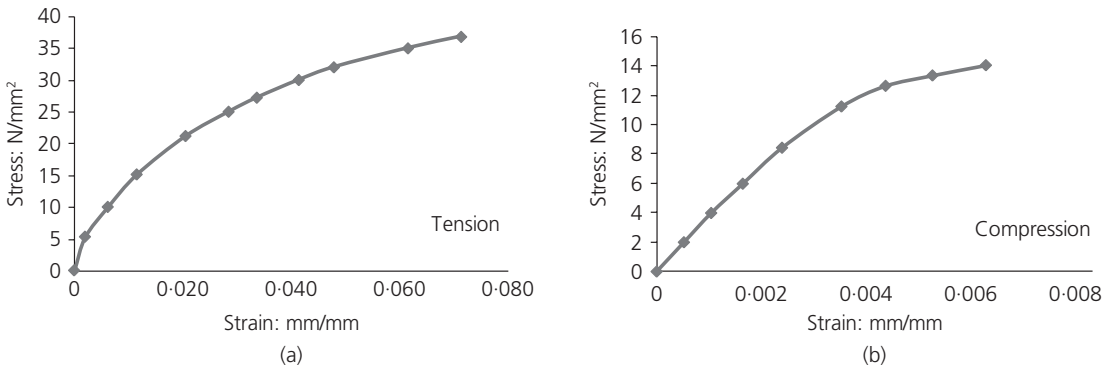

Figure 4. Typical stress–strain curves for (a) spruce in tension and (b) OSB in compression

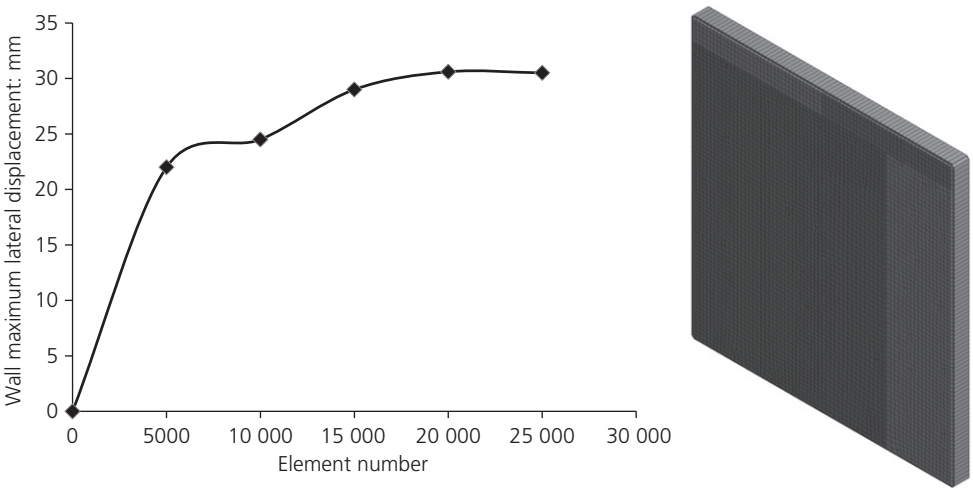

Figure 5. Mesh sizing optimisation study

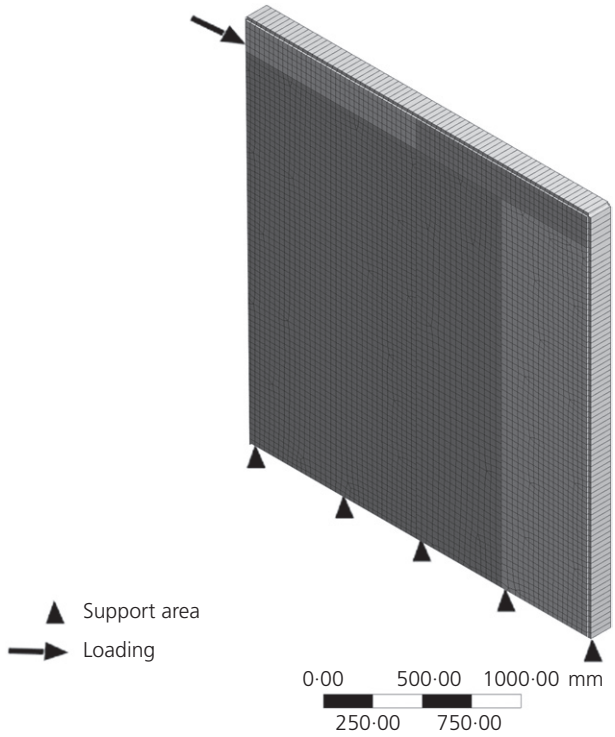

Figure 6. Loading and support mechanism of model

As shown in Figure 1, the test specimens were anchored to the rigid platform by specially designed U-shaped support plates. Each of these plates was connected to the rigid laboratory ground using five anchorages. As can be seen in Figure 1, the number of anchorage plates depended on the width of the panel wall. As the width of the timber-framed panel walls increased, the number of anchorage plates was also increased to obtain support conditions similar to the fixed-support assumption. In the simulation of the test specimens, as in the experiments, the panel walls were fixed in the regions of the anchorage plates (Figure 6). However, in the FE simulations, a variation in the number of support plates did not affect the fixed-support conditions. In the FE simulations, to have fixed-support conditions, it is necessary to constrain the related degrees of freedom. In contrast to the experimental study, a reduction in the number of anchorage plates leads to a deviation from the fixed-support condition. In relation to that, the maximum differences between experimental and numerical results were observed for specimen 8, which had the least number of anchorages.

4. Verification of numerical results

Finite-element analyses of 11 different wall panels were conducted. Static pushover analyses were conducted to compare the analytical and experimental load–deformation relationships.

The horizontal in-plane displacements of the test specimens and the deformations of the OSB surface covering plates were determined through equivalent stress analyses and the numerical results were compared with the experimental results (Figure 7). Good agreement between the analytical and experimental lateral displacements was observed, except for specimen 8, which showed the largest differences in the results. Specimen 8 had the smallest width and aspect ratio and hence behaved in a more ductile, flexure-dominant mode with pronounced displacement. Furthermore, in relation to its small width, the specimen was fixed at only two points, which led to significant rigid slip and rotation at the support region due to horizontal loading. Consequently, the numerical value of initial stiffness of specimens 8 is bigger than that of its experimental initial stiffness.

The stiffness of the analytical load–displacement relationships of panels with openings was observed to be larger than the

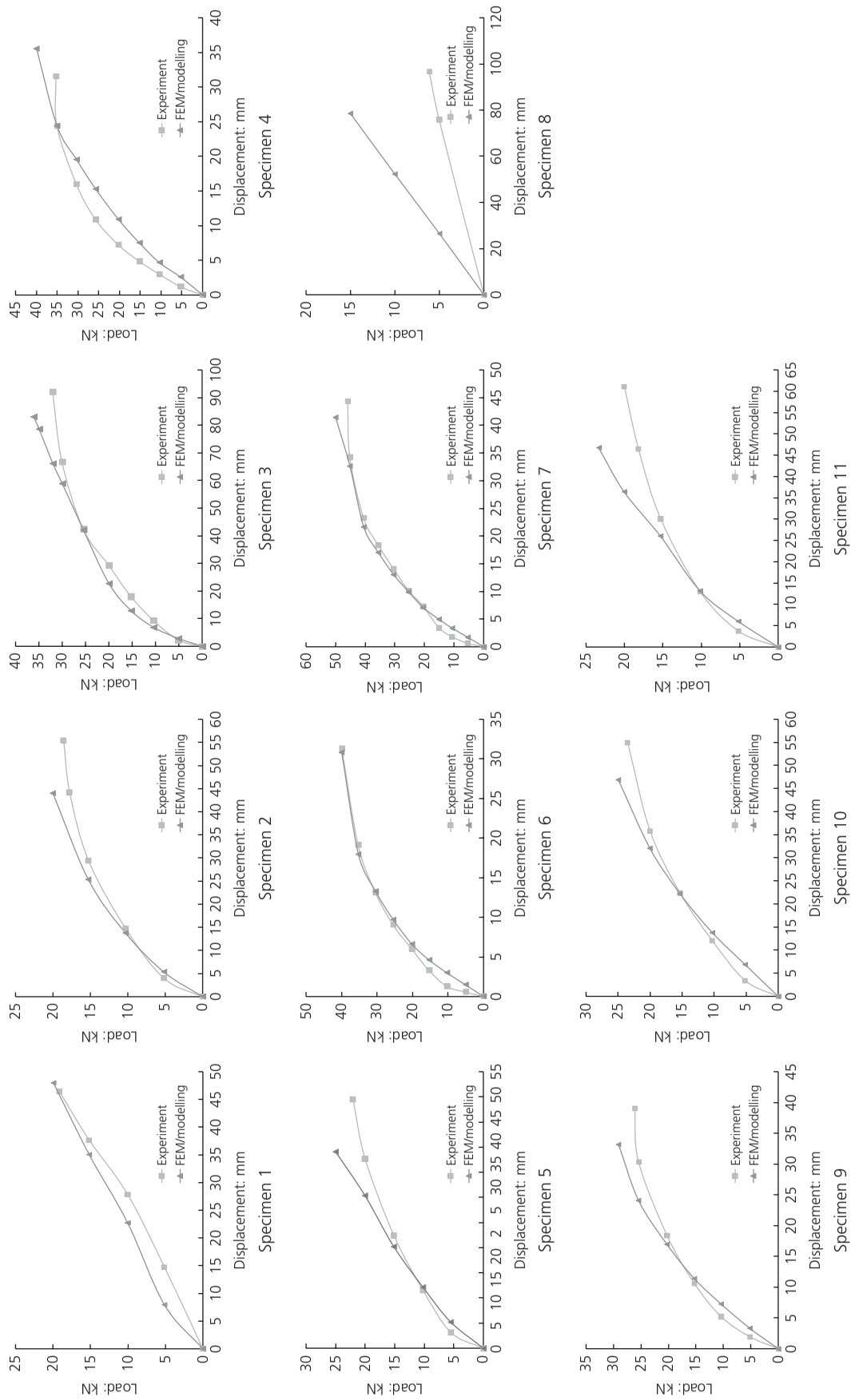

Figure 7. Comparison of numerical and experimental load–displacement curves under loading

experimental values. This difference may be attributed to the stiffer behaviour of the linking nails in the FE analysis. In contrast, the analytical and experimental results for panels without openings were in very good agreement (except specimen 8). The in-plane lateral displacement distributions observed in the panels under ultimate loads are given in Figure 8. In relation to the lower part of the panels being fully fixed to the rigid base, the deformations of the upper regions of the panels were larger than in the lower regions.

As expected, damage occurred in the panels due to increased loading levels. The level of damage under increased loading was obtained by stress analyses in the FE method (Loo *et al.*, 2012). The stress distributions in the OSB sheathing panel were determined under the ultimate load in the FE analyses (Figure 9). Figure 9 shows that the stress concentrations mainly occurred in the lower regions (with anchorages) and in the corners of the openings. The points of stress concentrations in the FE analyses were compared with the observation of damaged regions in the experimental study (Figure 10), and were found to be in good agreement. The experiments showed that the failure modes were a combination of nails pulling through the sheathing panels, tears in the OSB, sheathing panel edge tear-out and nail heads embedding into the panels.

5. Comparison of experimental and numerical results

The experimental and numerical results for the ultimate load capacity and corresponding ultimate displacement are given in Table 3. The average difference in ultimate load between the experimental and analytical results was 23%, with the analytical load-resisting capacities larger than the experimental ones. Similarly, the average difference in displacement at ultimate load between the experimental and analytical results was 10%, with the analytical deformations typically being smaller than the experimental values. In conclusion, it can be said that the FE analyses estimated the actual behaviour with significant accuracy. However, the stiffnesses of the numerical load–displacement relationships were observed to be larger than the experimental load–deformation relationships. The OSB plates used to sheet the timber frames were separately modelled (i.e. part by part) in real dimensions and the use of 'one large part in modelling' was avoided. This difference may be attributed to the following factors.

- In the FE analyses, the nails used in the frame connections were not modelled, resulting in a stiffer behaviour than the real behaviour. This is due to the fact that the frame members lose their initial stiffness with increased levels of loading. In relation to this point, the results in the elastic range were quite accurate but, with increased levels of loading, such accuracy was not found.
- From a comparison of the results obtained for panels with openings, the accuracy of the FE analyses was 84% on average. The higher displacement levels of panels with openings compared with panels without openings can be seen in Table 3. This behaviour may be attributed to the increased non-linearity of the frame and panel connections under increased loading. As stated before, the shear stiffness of the nails in the plastic region was calculated according to Eurocode5 (612 N/mm). This shear stiffness value was found to be smaller than the value required for estimating actual behaviour. This means that the nails exhibited softer behaviour, resulting in the observed differences in the load–displacement curves. On the other hand, the differences in the ultimate load capacities were quite small.
- Another important factor that may cause discrepancy is the boundary conditions. In the experiments, deformations were observed at the support locations. However, in the FE analyses, these deformations were prevented by using fixed boundary conditions in the support regions. Accordingly, preventing such a discrepancy was unavoidable.

6. Finite-element analyses performed on panels without experimental results

In this section, the FE analyses of panels without experimental results are presented. These panels were wider than the experimentally tested panels. The panel models were constructed with window and door openings to observe the effect of openings on the behaviour. The dimensions of the four timber panels analysed using the verified FE model are chosen based on the dimensions of real (large-scale) timber panels with door and window openings. The presence of single or multiple openings was also considered in the selection of dimensions. The panel dimensions were selected to give information to design engineers in practice (i.e. the largest dimensions in actual timber structures).

Yasumura and Sugiyama (1984) proposed equations to determine the strength and stiffness ratio (F), the opening area ratio (α), the wall length ratio (β) and the opening coefficient (r) (Equations 5–8).

5. $$F = \frac{r}{3 - 2r}$$

6. $$\alpha = \frac{A_0}{HL}$$

7. $$\beta = \frac{\sum_{\mathrm{i}}^{L}}{L}$$

8. $$r = \frac{1}{1 + (\alpha/\beta)}$$

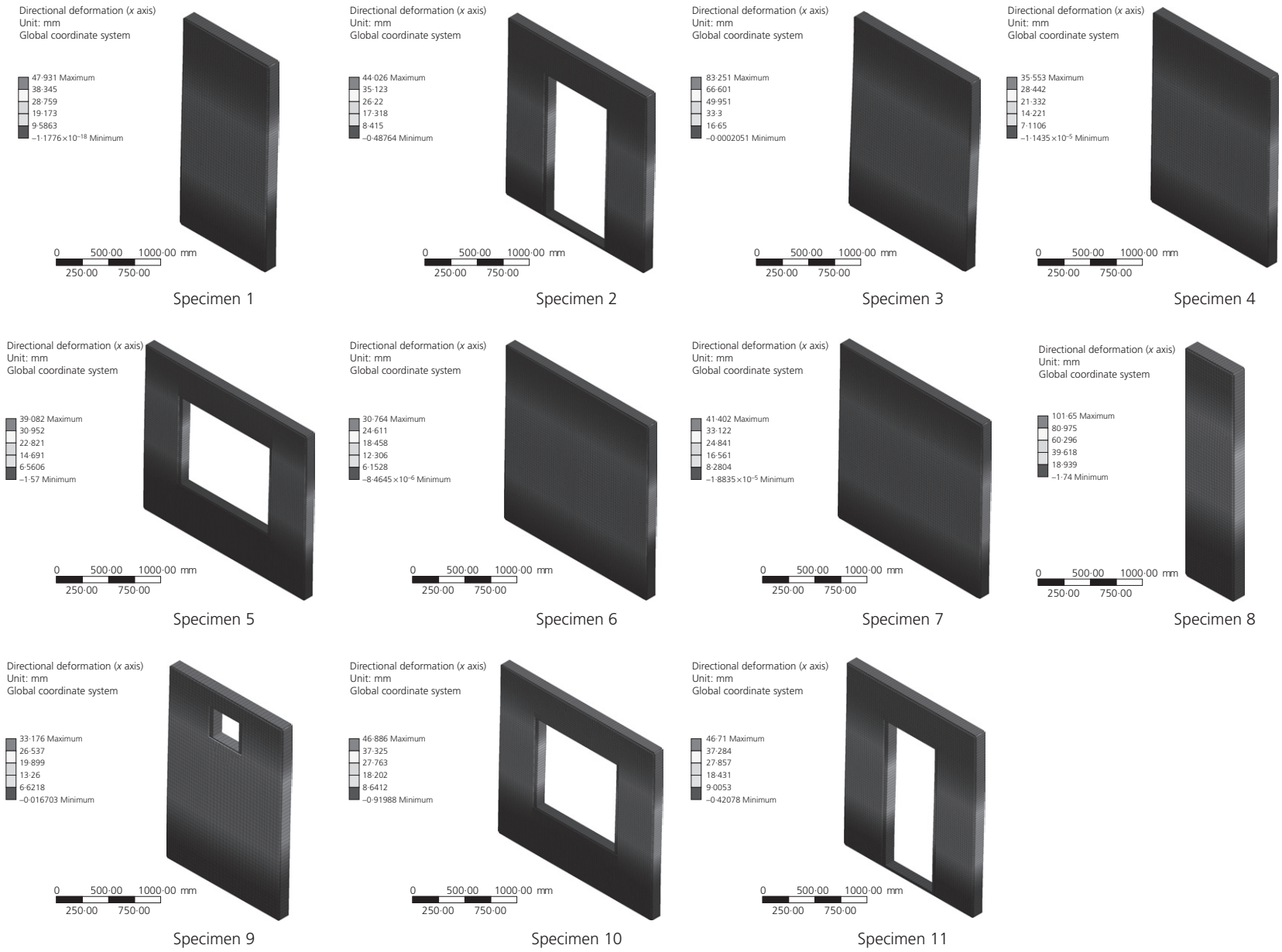

Figure 8. Contour plots of lateral displacements of wood-framed shear walls at ultimate load

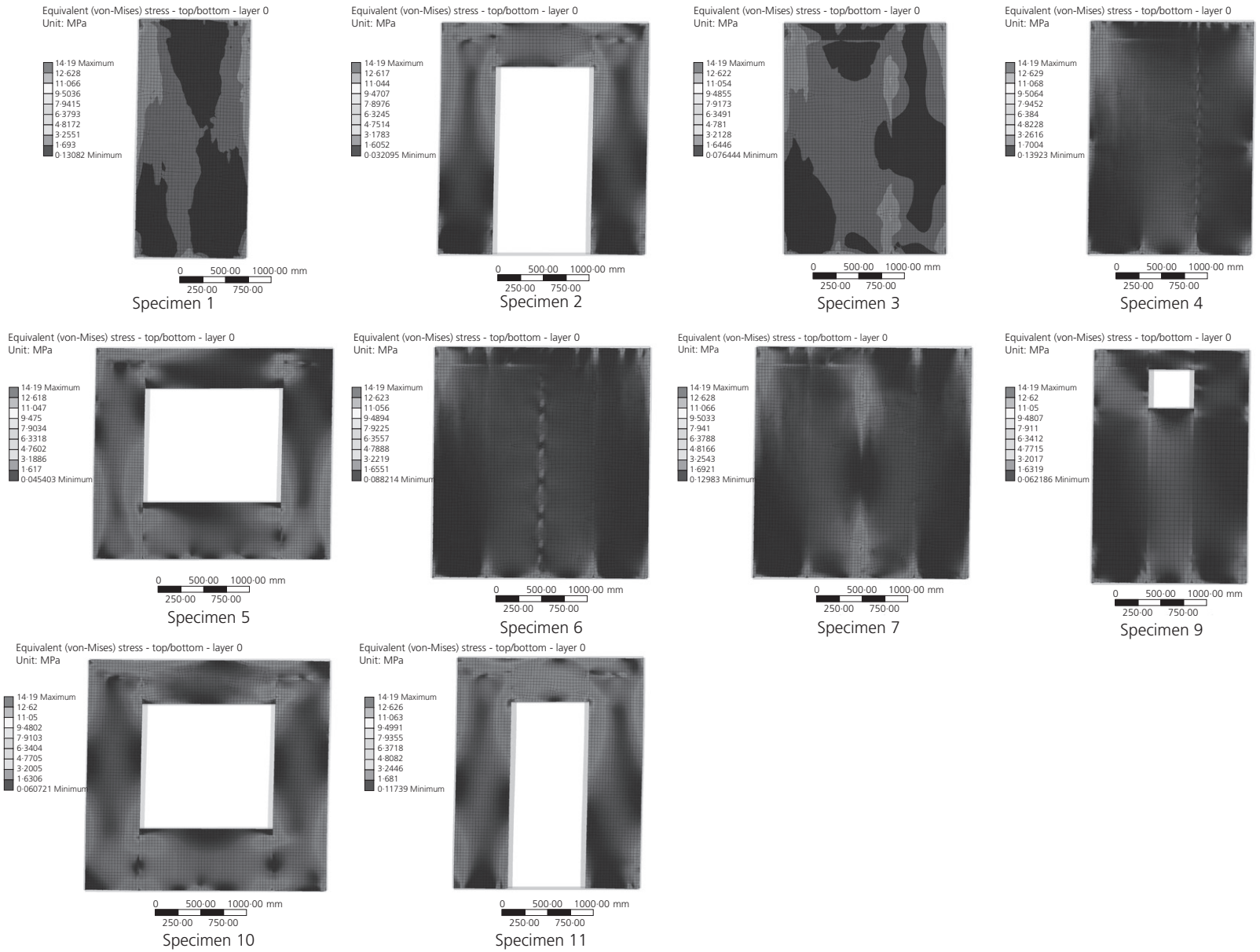

Figure 9. Stress distribution in the OSB sheathing panels at ultimate load

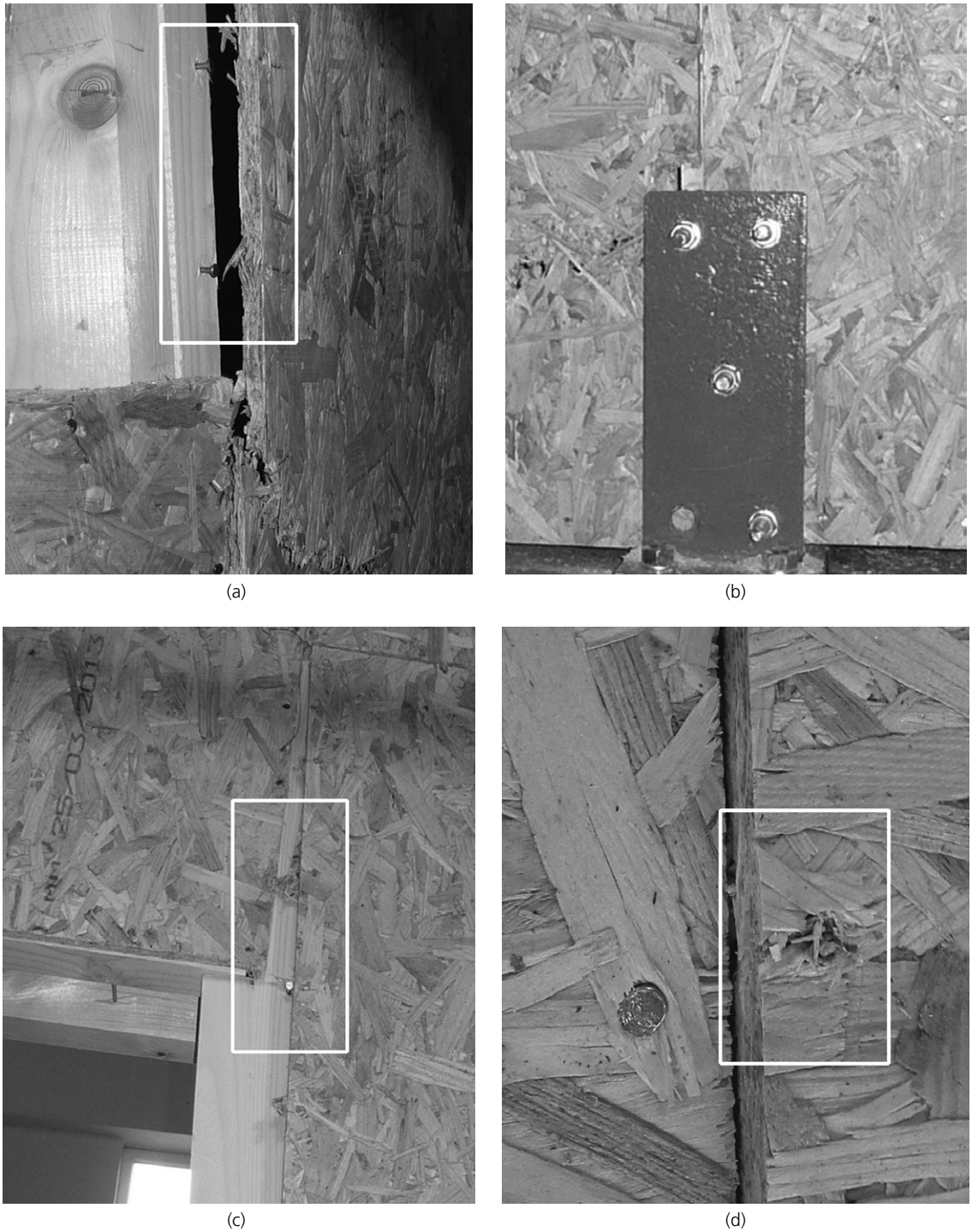

Figure 10. Damage observed in specimens after testing: (a) nails pulled through sheathing panel; (b) shear crack in OSB panel; (c) panel edge tear-out; (d) nail head embedded into panel

These calculated panel properties are listed in Table 4 for each of the four models. The table shows that the dimensions of the openings affect the panel strength. As expected, an increase in opening dimensions reduced the load-resisting capabilities.

The FE analyses of these wall panels were performed under horizontal loading conditions. The loading was applied with the implementation of 10 kN incremental steps. The parameters of the validated FE models were also used in these analyses.

Table 3. Comparison of experimental and numerical results

	Ultimate load			Displacement		
Specimen	Experimental: kN	Numerical: kN	Exp./num.	Experimental: mm	Numerical: mm	Exp./num.
1	19·16	20	0·96	46·40	47·93	0·97
2	18·59	20	0·93	55·46	44·02	1·26
3	32·05	36·2	0·89	92·02	83·25	1·11
4	35·27	40	0·88	31·57	35·55	0·89
5	22·10	25	0·88	49·44	39·08	1·27
6	39·89	40	1·00	31·29	30·76	1·02
7	45·87	50	0·92	44·37	41·40	1·07
8	6·09	15	0·41	96·64	78·49	1·23
9	26·13	29·1	0·90	39·03	33·17	1·18
10	23·55	25	0·94	54·95	46·88	1·17
11	20·02	23·3	0·86	61·07	46·71	1·31

Table 4. Panel properties calculated using the equations proposed by Yasumura and Sugiyama (1984)

Model	Timber wall width/height: mm	Door width/height: mm	Window width/height: mm	Opening area ratio, α	Wall length ratio, β	Opening coefficient, r	Strength ratio, F
1	4314/2650	900/2100	1500/1200	0·32	0·44	0·58	0·31
2	4314/2650	900/2100	—	0·17	0·79	0·83	0·61
3	4314/2650	—	1200/1500	0·16	0·65	0·81	0·58
4	4314/2650	—	676/ 1200	0·07	0·84	0·92	0·80

The distributions of deformation in the new FE analyses are shown in Figure 11 and the load–displacement relationships of the new FE analyses are given in Figure 12. From Figure 12, it can be seen that model 4 with a narrow window opening resisted a larger horizontal load (80 kN) than the other panels. Models 2 and 3 had similar opening dimensions and resisted similar horizontal loads (60 kN). Model 1, with the largest opening dimensions, resisted the smallest horizontal load (40 kN).

The relation between opening area ratio and load-resisting capacity is plotted in Figure 13 to give a better understanding of the effect of openings on the load-resisting capacities of timber-framed panel walls. Figure 13 shows that the coefficient of determination obtained from a linear curve fitting ($R^2 = 0{\cdot}960$) is very close to one. Figure 13 illustrates that an increase in opening area ratio linearly decreases the horizontal load resistance capacity of timber-framed panel walls. This relation may be of help to designers.

7. Conclusions

Timber-framed shear wall elements of different configurations were modelled using FE analyses. The frame elements were modelled as beams, the plates were modelled as shells and nails were modelled as spring elements to provide a fast and accurate analysis procedure. The numerical and experimental results were compared in the scope of this study, and good agreement was observed. Furthermore, the FE analyses of four further panels (without experimental results) were presented. The equations proposed by Yasumura and Sugiyama (1984) were used to investigate the effect of the presence of openings on panel strength and it was observed that the presence of openings significantly affects the load-resisting capacity. It was also found that the strength of the panels decreases with an increase in opening area ratio.

The behaviour of the timber-framed panels was significantly affected by the behaviour of the nails. In the FE analyses, the stiffness of the nails was calculated as per Eurocode 5, and the nails between the frame elements and panels were modelled as spring elements. However, these stiffness values resulted in a 10% difference from the experimental values. An evaluation of the stress distributions showed that the stress concentrations in the FE analyses were in the damaged regions in the experimental study.

In conclusion, good agreement between the numerical and experimental results was observed. In addition, it was found that the presence of openings significantly affects the load-resisting capacity of timber-framed panels. The number of data points was increased by conducting additional FE analyses in order to develop an equation to show the effect of openings on the horizontal load resistance capacity of timber-framed panels. From linear curve fitting of the data it was concluded that such an equation may help designers.

Acknowledgements

This study (01332STZ.2012-1 San-Tez project) was supported by the Ministry of Science, Industry and Technology. The

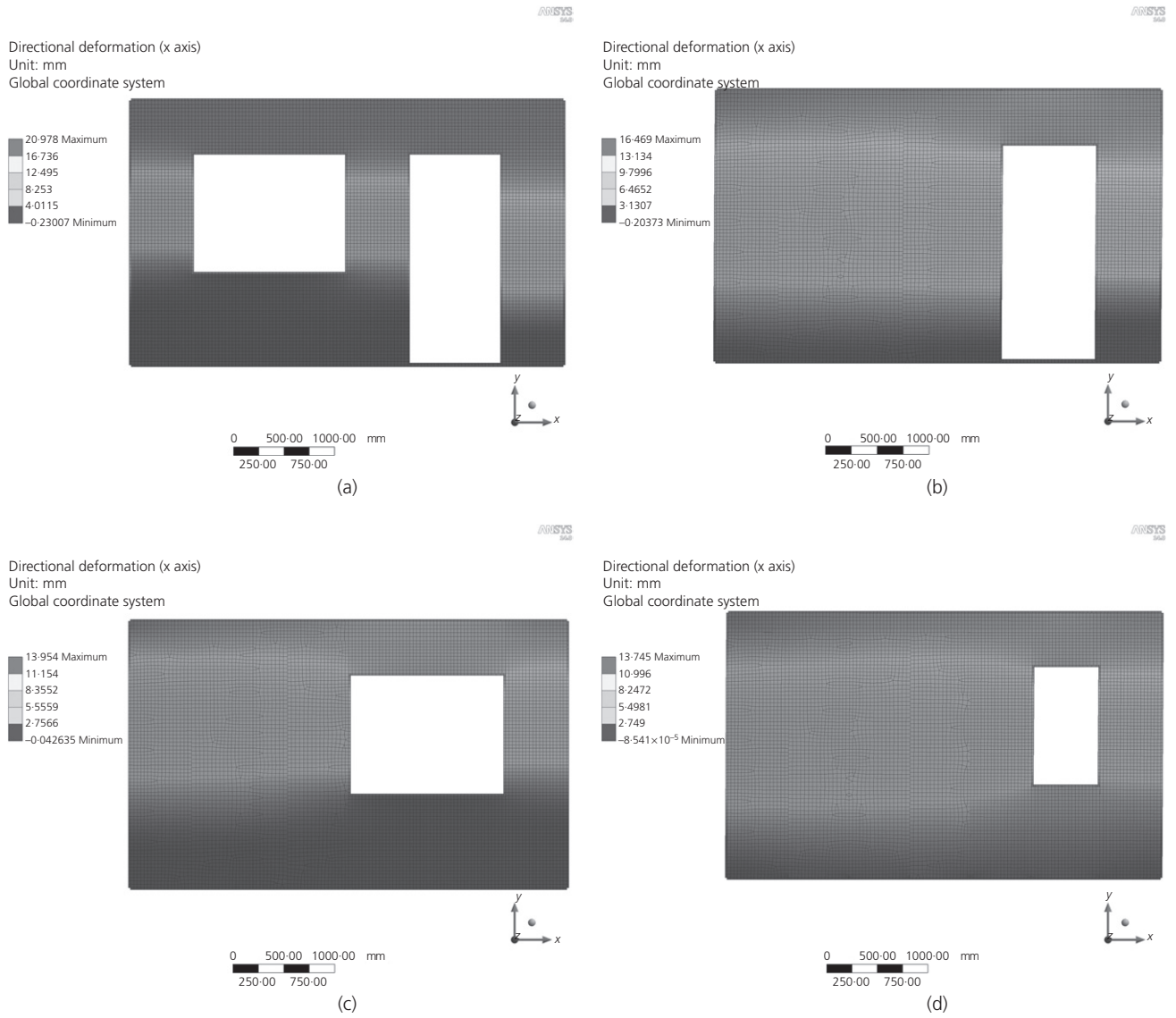

Figure 11. FE analysis of different timber-framed shear walls: (a) model 1; (b) model 2; (c) model 3; (d) model 4

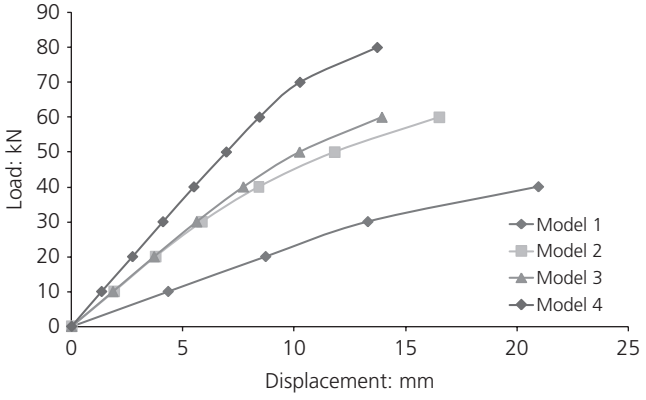

Figure 12. Comparison new wall model load–displacement curve

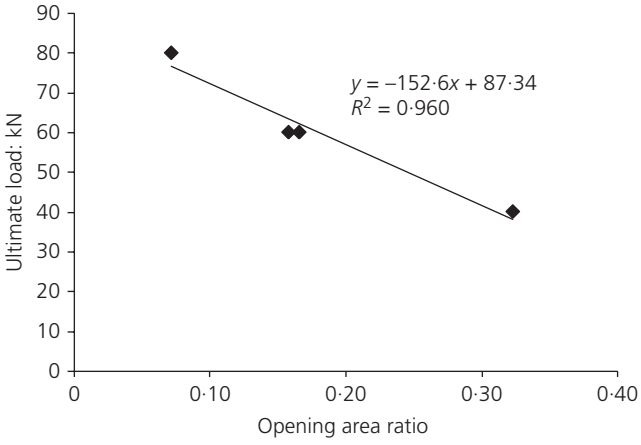

Figure 13. Variation of ultimate load with opening area ratio

authors express their gratitude to the ministry and to Şanver Furniture, Decoration, Construction Forest Products Corporation for their support of the project.

REFERENCES

Andreasso S, Yasumura M and Daudeville L (2002) Sensitivity study of the finite element model for wood-framed shear walls. *Journal of Wood Science* **48(3)**: 171–178.

Anıl Ö, Togay A, Karagöz Ü, Söğütlü C and Döngel N (2016) Hysteretic behavior of timber framed shear wall with openings. *Construction and Building Materials* **116**: 203–215, http://doi.org/10.1016/j.conbuildmat.2016.04.068.

ASTM (2011) ASTM D3501-05a: Standard test methods for wood-based structural panels in compression. ASTM International, West Conshohocken, PA, USA.

Ayoub A (2007) Seismic analysis of wood building structures. *Engineering Structures* **27(2)**: 213–223.

Baylor G and Harte AM (2013) Finite element modelling of castellated timber I-joists. *Construction and Building Materials* **47**: 680–688, http://doi.org/10.1016/j.conbuildmat.2013.05.076.

Blasetti AS, Hoffman R and Dinehart D (2008) Simplified hysteresis finite-element model for wood and viscoelastic polymer connections for the dynamic analysis of shear walls. *Journal of Structural Engineering* **134(1)**: 77–86.

Bolmsvik A, Linderholt A, Brandt A and Ekevi T (2014) FE modelling of light weight wooden assemblies – parameter study and comparison between analyses and experiments. *Engineering Structures* **73**: 125–142, http://doi.org/10.1016/j.engstruct.2014.04.028.

Boudaud C, Humbert J, Baroth J, Hameury S and Daudeville L (2015) Joints and wood shear walls modelling II: experimental tests and FE models under seismic loading. *Engineering Structures* **101**: 743–749, http://doi.org/10.1016/j.engstruct.2014.10.053.

Casagrande D, Rossi S, Sartori T and Tomasi R (2016) Proposal of an analytical procedure and a simplified numerical model for elastic response of single storey timber shear-walls. *Construction and Building Materials* **102**: 1101–1112, http://doi.org/10.1016/j.conbuildmat.2014.12.114.

CEN (European Committee for Standardization) (2010) EN 1995-1-1: Eurocode 5: Design of timber structures – part 1–1: general – common rules and rules for buildings. CEN, Brussels, Belgium.

Folz B and Filiatrault A (2001) Cyclic analysis of wood shear walls. *Journal of Structural Engineering ASCE* **127(4)**: 433–441.

Foschi RO (1977) Analysis of wood diaphragms and trusses part I: diaphragms. *Canadian Journal of Civil Engineering* **4(3)**: 345–352.

Guan ZW and Zhu EC (2009) Finite element modelling of anisotropic elasto-plastic timber composite beams with openings. *Structures* **31**: 394–403, http://doi.org/10.1016/j.engstruct.2008.09.007.

Humbert J, Boudaud C, Baroth J, Hameury S and Daudeville L (2014) Joints and wood shear walls modelling I: constitutive law, experimental tests and FE model under quasi-static loading. *Engineering Structures* **65**: 52–61, http://doi.org/10.1016/j.engstruct.2014.01.047.

Judd JP and Fonseca FS (2005) Analytical model for sheathing-to-framing connections in wood shear walls and diaphragms. *Journal of Structural Engineering* **131(2)**: 345–352.

Källsner B and Girhammar U (2009) Analysis of fully anchored light-frame timber shear walls-elastic model. *Materials and Structures* **42(3)**: 301–320.

Loo WY, Quennevillea P and Chouw N (2012) A numerical approach for simulating the behavior of timber shear walls. *Structural Engineering and Mechanics* **42(3)**: 383–407.

Meghlat EM, Oudjene M, Ait-Aider H and Batoz JL (2013) A new approach to model nailed and screwed timber joints using the finite element method. *Construction and Building Materials* **41**: 263–269, http://doi.org/10.1016/j.conbuildmat.2012.11.068.

Pang W and Rosowsky D (2010) Beam-spring model for timber diaphragm and shear walls. *Structures and Buildings* **163(SB4)**: 227–244.

Pintaric K and Premrov M (2013) Mathematical modelling of timber-framed walls using fictive diagonal elements. *Applied Mathematical Modelling* **37(16–17)**: 8051–8059.

Polensek A (1976) Finite-element analysis of wood-stud walls. *Journal of the Structural Division ASCE* **102(7)**: 1317–1335.

Premrov M and Dobrila P (2012) Numerical analysis of sheathing boards influence on racking resistance of timber-frame walls. *Advances in Engineering Software* **45(1)**: 21–27.

Premrov M and Kuhta M (2008) Influence of fasteners disposition on behavior of timber frame walls with single fibre-plaster sheathing boards. *Construction and Building Materials* **23(7)**: 2688–2693.

Premrov M and Kuhta M (2010) *Experimental Analysis on Behaviour of Timber-framed Walls with Different Types of Sheathing Boards, Construction Materials and Engineering*. Nova Science, Hauppauge, NY, USA.

Richard N, Daudeville L, Prion H and Lam F (2002) Timber shear walls with large openings: experimental and numerical prediction of the structural behavior. *Canadian Journal of Civil Engineering* **29(5)**: 713–724.

Šilih EK, Premrov M and Šilih S (2012) Numerical analysis of timber-frame d wall elements coated with single fibre-plaster boards. *Engineering Structures* **41**: 118–125, http://doi.org/10.1016/j.engstruct.2012.03.044.

TSE (Turkish Standards Institution) (1976) TS 2475: Wood-determination of ultimate tensile stress parallel to grain. TSE, Ankara, Turkey.

Valipour H, Khorsandnia N, Crews K and Foster S (2014) A simple strategy for constitutive modelling of timber. *Construction and Building Materials* **53**: 138–148, http://doi.org/10.1016/j.conbuildmat.2013.11.100.

Xu J and Dolan JD (2009a) Development of a wood-frame shear all model in Abaqus. *Journal of Structural Engineering* **135(8)**: 977–984.

Xu J and Dolan JD (2009b) Development of nailed wood joint element in Abaqus. *Journal of Structural Engineering* **135(8)**: 968–976.

Xu BH, Bouchair A and Racher P (2012) Analytical study and finite element modelling of timber connections with glued-in rods in bending. *Construction and Building Materials* **34**: 337–345, http://doi.org/10.1016/j.engstruct.2014.01.047.

Yasumura M and Sugiyama H (1984) Shear properties of plywood-sheathed wall panels with opening. *Transactions of the Architectural Institute of Japan* **338(4)**: 88–98.

Zhu EC, Guan ZW, Rodd PD and Pope DJ (2005) A constitutive model for OSB and its application in finite element analysis. *HolzRohWerkst* **63(2)**: 87–93.

How can you contribute?

To discuss this paper, please email up to 500 words to the editor at journals@ice.org.uk. Your contribution will be forwarded to the author(s) for a reply and, if considered appropriate by the editorial board, it will be published as discussion in a future issue of the journal.

Proceedings journals rely entirely on contributions from the civil engineering profession (and allied disciplines). Information about how to submit your paper online is available at www.icevirtuallibrary.com/page/authors, where you will also find detailed author guidelines.